Genetic and physiological insights into the diazotrophic activity of a non-cyanobacterial marine diazotroph

Aurélie Joublin-Delavat[1], Katia Touahri[1,2], Amandine Morot[3,4], Sophie Rodrigues[4], Bruno Jesus[5], Florian Trigodet and François Delavat*[,1]

[1] Nantes Université, CNRS, US2B, UMR6286, F-44000 Nantes, France
[2] Laboratoire Chimie et Biochimie de Molécules Bioactives, Université de Strasbourg/CNRS, UMR7177, F-67081 Strasbourg, France
[3] Univ Brest, CNRS, IRD, Ifremer, LEMAR, F-29280 Plouzané, France
[4] Université de Bretagne-Sud, UR3884, LBCM, IUEM, F-56100 Lorient, France
[5] Nantes Université, RSBE[2] ISOMer, UR2160, F-44000 Nantes, France
[6]The University of Chicago, Department of Medicine , Chicago, Illinois, USA
* corresponding author: francois.delavat@univ-nantes.fr

Abstract

Nitrogen (N_2) fixation, or diazotrophy, supports a large part of primary production in oceans. Culture-independent approaches highlighted the presence in abundance of marine non-cyanobacterial diazotrophs (NCD) but their ecophysiology remains elusive, mostly because of the low number of isolated NCD and because of the lack of available genetic tools for these isolates. Here, a dual genetic and functional approach allowed unveiling the ecophysiology of a marine NCD affiliated to the species *Vibrio diazotrophicus*. Physiological characterization of the first marine NCD mutant obtained so far was performed using a soft-gellan assay, demonstrating that a Δ*nifH* mutant in not able to grow in nitrogen-deprived media. Furthermore, we demonstrated that *V. diazotrophicus* produces a thick biofilm under diazotrophic conditions, suggesting biofilm production as an adaptive response of this NCD to cope with the inhibition of nitrogen-fixation by molecular oxygen. Finally, the genomic signature of *V. diazotrophicus* is essentially absent from metagenomic data of *Tara Ocean* expeditions, despite having been isolated from various marine environments. We think that the genetically tractable *V. diazotrophicus* strain used in this study may serve as an ideal model to study the ecophysiology of these overlooked procaryotic group.

Introduction

Nitrogen is a macro-element essential for life, as it is found in many biological molecules (*i.e.* nucleic acids, proteins). The atmosphere is composed by 78% of dinitrogen (N_2) but this form cannot be assimilated by the vast majority of the organisms. The process of N_2 fixation or diazotrophy is pivotal in oceanic ecosystems, since it makes the newly fixed nitrogen accessible to the entire plankton community, fueling primary production (Tang et al., 2019). Diazotrophy is now considered a key player in the biogeochemical cycles of nitrogen, but also of carbon, since it stimulates the biological pump, a mechanism absorbing a significant portion of the carbon dioxide emitted into the atmosphere and exporting it to the ocean seafloor. Diazotrophy is particularly crucial in tropical and subtropical area, where oceanic primary production is typically limited by the limited dissolved inorganic nitrogen (DIN) bioavailability (Capone et al., 2005). In addition, recent *in situ* quantification of N_2 fixation demonstrated high diazotrophic activity in DIN-replete marine environments (Mulholland et al., 2019; Tang et al., 2019), showing the overall importance of diazotrophy in oceans.

Diazotrophy is an anabolic process restricted to some prokaryotic species (found both in *Bacteria* and *Archaea*). *Cyanobacteria* like the free-living *Trichodesmium* are known since decades to be important oceanic nitrogen fixers (Carpenter and Romans, 1991), accounting for at least 1.6 Tmol N in the tropical North Atlantic alone (Capone et al., 2005). Other *Cyanobacteria*, typically living in symbiotic association with photosynthetic microalgae also contribute significantly. These associations include diatom-diazotroph associations (DDA), where filamentous *Cyanobacteria* like *Richelia intracellularis* and *Calothrix rhizosoleniae* can be located either intra- or extracellularly to fix N_2 and transfer the newly fixed nitrogen to sustain diatom growth (Nieves-Morion et al., 2020), receiving organic carbon from its host in return (Foster et al., 2022). DDA associations can account for 0.19 and 0.62 Tmol N per year in Atlantic and Pacific oceans, respectively (Foster et al., 2011). Another example includes the unicellular cyanobacterial lineage UCYN-A, which associate with haptophytes and fixes N_2 even under nitrogen-replete conditions (Mills et al., 2020) and which significantly contribute to N_2 fixation in oceans (Martinez-Perez et al., 2016).

Despite the tremendous data related to cyanobacterial N_2-fixation in oceans, the global N budget in frequently considered unbalanced, as the N loss by denitrification and anammox largely exceeds N input (Landolfi et al., 2018). This suggests that alternative players are

missing to equilibrate the N budget. More and more evidence show the presence in all oceans of previously overlooked nitrogen-fixers, not affiliated to the phylum *Cyanobacteria*. Indeed, culture-independent approaches based on the amplification or immunodetection of the *nifH* gene, a gene encoding a subunit of the nitrogenase, conserved among diazotrophs and considered as a biomarker for diazotrophy, have demonstrated the presence of marine Non-Cyanobacterial Diazotrophs (NCDs) (Zehr et al., 1998) in the water column attached to particles (undefined aggregates, faecal pellets) (Farnelid et al., 2019; Geisler et al., 2019) and in deep sea sediments (Kapili et al., 2020). Moreover, *Tara Oceans* expeditions provide metagenomic data from diverse oceanic locations, depths and size fractions, coupled with physical and chemical information (Karsenti et al., 2011; Planes et al., 2019). Analyses of the metagenomes allowed the reconstructions of MAGs (Metagenome-Assembled Genomes) from diverse diazotrophs, including many NCDs, found in abundance in diverse oceans (Delmont et al., 2018; Delmont et al., 2022). Metatranscriptomic analysis from *Tara Oceans* data showed that many NCDs express their *nifH* gene and are therefore active (Delmont et al., 2022).

From a biochemical point of view, diazotrophic activity faces a strong metabolic constraint under oxic conditions (Gallon, 1992). Indeed, O_2 acts at different levels to block diazotrophy: it can (i) inhibit the synthesis of *nif* genes including *nifH* (Hubner et al., 1991; Dixon and Kahn, 2004), (ii) lead to irreversible damages of the nitrogenase (Gallon, 1992), and (iii) reversibly inhibit the nitrogenase activity (Goldberg et al., 1987). This O_2-based inhibition of diazotrophy poses a metabolic conundrum, since many diazotrophs are also aerobes and therefore use O_2 as a terminal electron acceptor for aerobic respiration. To solve this dilemma, terrestrial diazotrophs committed to symbiotic interactions with legume roots (and sometimes on stems (Bonaldi et al., 2011)) are engulfed within a plant organ called nodule. This nodule serves as a physical barrier, limiting O_2 diffusion and creating micro-aerobic environments where both nitrogen fixation and respiration co-occur. Other terrestrial diazotrophs, like the free-living diazotroph *Azotobacter vinelandii* produces a cytochrome *bd* terminal oxidase, that consumes a high volume of O_2, which leads to a rapid decrease in intracellular O_2-tension, allowing nitrogen fixation in overall aerobic environments (Kelly et al., 1990; Poole and Hill, 1997). Additionally, *A. vinelandii* secretes an alginate capsule, which thickness increases with O_2 tension and which serves as a barrier for O_2 diffusion into the cells (Sabra et al., 2000).

102 In addition to the O_2 tension found in oceans, marine *Cyanobacteria* face another challenge
103 when regarding nitrogen fixation, since many of them are photosynthetic and release O_2 as a
104 byproduct of oxygenic photosynthesis. Marine *Cyanobacteria* have therefore also developed
105 various strategies to solve this metabolic constraint. Free-living filamentous *Cyanobacteria*
106 like *Anabaena* sp. (Zhang et al., 2006), but also those living in symbiotic associations with
107 photosynthetic diatoms like *R. intracellularlis* and *C. rhizosoleniae* (Foster et al., 2011)
108 phenotypically differentiate into distinct subpopulations: when DIN becomes limiting, some
109 cells within the filament specialize in nitrogen-fixing factories. These cells, called heterocysts
110 have a modified envelope containing additional layers (a glycolipid and a polysaccharide
111 layer) which restricts O_2 diffusion in the cell cytoplasm (for a review, see (Flores et al.,
112 2019)). Heterocysts commit to a dedicated developmental program (Flores et al., 2019), also
113 marked by the loss of ability to perform oxygenic photosynthesis, which is restricted to the
114 neighboring vegetative cells (Zhang et al., 2006). Molecular exchanges of nitrogen and
115 carbon compounds therefore occur between the vegetative cells and the heterocysts to
116 sustain the growth of the filament (Nieves-Morion et al., 2021). As an alternative to this
117 spatial regulation of diazotrophy, some unicellular *Cyanobacteria* like *Crocosphaera* perform
118 oxygenic photosynthesis during the day and nitrogen fixation during the night (Tuit et al.,
119 2004). Finally, non-heterocyst diazotrophs may protect their nitrogenase from O_2 by the
120 production of hopanoid lipids (Cornejo-Castillo and Zehr, 2019).
121 In contrast, while strategies deployed by marine cyanobacterial diazotrophs to perform
122 nitrogen fixation in oxic environment are documented, knowledge on those for marine NCD
123 remain understudied (Bombar et al., 2016). This knowledge gap is due to the limited number
124 of NCD isolated from marine environments (Farnelid et al., 2014; Martinez-Perez et al.,
125 2018). Additionally, their physiology remains elusive because, to our knowledge, no genetic
126 mutant of marine NCD has been obtained so far, hampering an in-depth physiological
127 characterization of marine NCD.
128 *Vibrio diazotrophicus* is a marine bacterium, firstly isolated from gastrointestinal tract of sea
129 urchins (Guerinot and Patriquin, 1981). It can be found in marine and estuarine
130 environments (Guerinot et al., 1982) as well as in sediments (Castillo et al., 2018) and in
131 enriched marine phytoplankton exometabolites (Fu et al., 2020). The type strain *V.*
132 *diazotrophicus* NS1 (ATCC 33466) was shown by acetylene reduction assay (ARA) to produce
133 nitrogenase and fix N_2 (Guerinot and Patriquin, 1981). The genome of *V. diazotrophicus* NS1

134 is available (accession number BBJY00000000.1, no associated publication or genomic
135 characterization) and other isolates have been fully sequenced (Castillo et al., 2018).
136 However, besides the description of its isolation in 1981 and its taxonomical characterization
137 one year latter (Guerinot et al., 1982), no further physiological or genetic characterization of
138 any member of this species has been performed. Because of its presence in various oceanic
139 environments and because many genetic and molecular tools are available for this genus
140 (Delavat et al., 2018; Morot et al., 2021), we think that *V. diazotrophicus* can constitute an
141 ideal model to assess the ecophysiology of marine NCD and their diazotrophic activity.
142 In this manuscript, we report the physiological description of *V. diazotrophicus* NS1, together
143 with the construction of the first genetic mutant of a marine NCD, impaired in nitrogen-
144 fixation. Importantly, we showed that under nitrogen-deficient conditions, *Vibrio*
145 *diazotrophicus* produces more biofilm, suggesting the role of biofilm as a barrier of O_2
146 diffusion.
147
148 **Material and Methods**
149
150 *Strains and culture conditions*
151 The strains, plasmids and primers used in this study can be found in Table S1, S2 and S3,
152 respectively. Unless otherwise stated, *V. diazotrophicus* NBRC 103148 and *Escherichia coli*
153 were grown in LB at 30°C and 37°C, respectively. The nitrogen-deficient media used in this
154 study is a modified diazotrophic medium for *Vibrio* (MDV), composed similarly to (Guerinot
155 and Patriquin, 1981), with the following modifications: solution 1 was prepared with NaCl
156 0.3 M, $MgSO_4$, $7H_2O$ (0.05 M), $CaCl_2$, $2H_2O$ (0.01 M), KCl (0.01 M), Tris (0.05 M) adjusted to
157 pH 7.5, before the addition of 0.3 $g.l^{-1}$ yeast extract. Solution 2 was prepared in 500 ml H_2O
158 with 0.005 g Na_2MoO_4, $2H_2O$, 40 g glucose, 1 ml of a 3 $g.l^{-1}$ FeNaEDTA,$3H_2O$ stock solution.
159 Solution 3 was prepared in 166 ml H_2O with 0.2 g KH_2PO_4 and 0.8 g K_2HPO_4 adjusted to pH
160 7.2. All 3 solutions were autoclaved, allowed to cool separately, and MDV was prepared by
161 mixing 333 ml of solution 1, 500 ml of solution 2 and 166 ml of solution 3. 1 ml of a vitamin
162 cocktail (stock solution containing 1 $mg.l^{-1}$ biotin, 1 $mg.l^{-1}$ vitamin B12 and 0.2 $g.l^{-1}$ thiamin-
163 HCl) was subsequently added to 1 l MDV.

164 If necessary, trimethoprim (Trim, 10 μg.ml^{-1}), kanamycin (Km, 50 μg.ml^{-1}), diaminopimelic
165 acid (DAP, 0.3 mM), glucose (0.3 g.l^{-1}), L-arabinose (L-ara, 0.2%) or agar (1.5%) were added
166 to the media.
167 Doubling times were determined by spectrophotometry using the TECAN Infinite M1000.
168 Briefly, one colony of each studied strain was inoculated in LB+Trim and incubated
169 overnight. The next morning, cells were washed 3 times to remove old LB from the overnight
170 culture, OD_{600nm} was adjusted to 0.01 with fresh LB, and 200 μl were used to inoculate 4
171 wells from a polystyrene plate (Dutscher, ref 330035). Plate was left in the TECAN
172 instrument set at 30°C without shaking, and OD_{600nm} was measured every 30 minutes for 48
173 hours. Doubling times were calculated from the exponential growth phase of each culture.
174
175 *Strain constructions and DNA techniques*
176 Standard procedures were used for all molecular techniques, following the reagent suppliers
177 recommendations. Deletion of *nifH* was performed by double homologous recombination
178 between a suicide plasmid and the chromosome of *V. diazotrophicus*, following a previously
179 established protocol (Morot et al., 2021), with some adaptations: *V. diazotrophicus* was
180 grown overnight at 30°C (it does not grow at 37°C), cointegrates were incubated in LB+L-ara
181 liquid before plating on LB+L-ara, and the temperature used to incubate the filter-deposited
182 LB+DAP plates was 30°C. The suicide plasmid pFD114 (Table S2) was constructed by
183 amplifying around 750 bp of the upstream and downstream regions of the *nifH* gene of *V.*
184 *diazotrophicus* (BBJY01_570151), using primers 210210 to 210213 (Table S3). Correct
185 deletion of *nifH* was verified using primers 210501 and 210502.
186 Complementation of *nifH* was achieved by amplifying the *nifH* gene and its dedicated
187 promoter, using primers 210204 and 210205 (Table S3). The P_{nifH}-*nifH* amplicon was cloned
188 within the pGEM-T vector (Promega), verified by sequencing and cloned within pFD086
189 (Morot et al., 2021) to replace P_{lac}-*gfp*, using BamHI and XhoI. The resulting pFD120 plasmid
190 was introduced by biparental mating as described above, using β3914 containing pFD120 as
191 a donor strain. All *in silico* plasmid maps are available upon request.
192 Electroporation assays were performed following an already published method (Delavat et
193 al., 2018), except the growing temperature of *V. diazotrophicus*, set at 30°C.
194
195 *Soft-gellan Assay*

196 This medium was prepared as follows (for one tube): 6.7 ml of solution 1 without yeast
197 extract plus 2 mg gellan gum were distributed in 18 cm glass tubes (Dutscher, ref 508232);
198 10 ml of solution 2 containing 3 mg gellan gum in a separate bottle; 3.33 ml of solution 3
199 containing 1 mg gellan gum in a separate bottle. All solutions were autoclaved separately,
200 allowed to cool to 45°C, mixed in the glass tube, gently homogenized by inversion, before
201 the addition of 20 µl of vitamin and Trim. If necessary, 20 µl of NO_3^- (stock solution $NaNO_3$ at
202 46.67 $g.l^{-1}$) were added together with vitamins and Trim after autoclave. If necessary, 20 mg
203 NH_4Cl were added in the 3.33 ml of solution 3 before autoclave.
204 *V. diazotrophicus* containing the empty plasmid pFD085 and *V. diazotrophicus* Δ*nifH*
205 containing either pFD085 or pFD120 were grown overnight in LB+Trim. 1 ml of overnight
206 cultures was subsequently washed with 1 ml nitrogen-free MDV (without yeast extract), and
207 pellets were resuspended with 500 µl nitrogen-free MDV. 100 µl of these washed
208 suspensions were used to inoculate the soft-gellan tubes and tubes closed with a sterile blue
209 rubber stopper, mixed by inversion and before being sealed with an aluminum capsule.
210 Tubes were left for incubation at room temperature for 48 hours. The experiment was
211 performed in triplicates.
212 Dissolved O_2 concentrations were measured with a retractable fiber oxygen microsensor (tip
213 diameter 50-70 µm, OXR50-OI, Pyro Science GmbH, Germany). The oxygen microsensor was
214 connected to a FireSting-O_2 fiber-optic oxygen meter (FireSting-O_2, Pyro Science GmbH,
215 Germany) and signals were recorded with a PC via the software Pyro Oxygen Logger (v3.319,
216 Pyro Science GmbH, Germany). The sensor was linearly calibrated in distilled water by
217 measuring in aerated water (100%) and in the same medium, in which 200 µl of Hcl-cysteine
218 (5 %) was added after media preparation to reduce any trace of O_2 (0%). The position of the
219 sensor was controlled by a micromanipulator (MU1, Pyro Science, GmbH, Germany).
220 Measurements were done before the medium-air interface and at the location of the
221 bacterial ring.
222
223
224 *Biofilm production in microplates*
225 Strains carrying either pFD085 or pFD120 were inoculated from a single colony in 5 ml
226 LB+Trim and incubated overnight at 30°C with shaking. Part of the cultures were washed 3
227 times with LB, diluted to an initial OD_{600nm} of 0.01 with LB+Trim, and 200 µl of this OD-

228 adjusted suspension were inoculated in quadruplicate in a 96-polystyrene-well microplate
229 (Dutscher, ref 330035). The remaining overnight cultures were washed 3 times with MDV,
230 adjusted to an initial OD_{600nm} of 0.01 with MDV+Trim, with MDV+Trim containing 46,67 $mg.l^{-1}$
231 NO_3^- or with MDV+Trim containing 20 $mg.l^{-1}$ NH_4Cl, and 200 µl of these OD-adjusted
232 suspensions were inoculated in quadruplicate in the same microplate. Plates were placed in
233 a microplate reader (TECAN Infinite M1000) for 48 hours at 30°C without shaking, and
234 OD_{600nm} was measured every 30 minutes. After 48 hours, plates were treated following an
235 already established protocol (Morot et al., 2021). Biofilm production was corrected by
236 dividing the OD_{550nm} measured after crystal violet staining by the maximal OD_{600nm} measured
237 during the growing time of the corresponding well.
238
239 *Biofilm production on flowcells*
240 *V. diazotrophicus* biofilms were grown at 30°C under hydrodynamic conditions in a three-
241 channel flow cell (1 x 4 x 44 mm; Biocentrum, DTU, Denmark (Pamp et al., 2009)). The flow
242 system was assembled, prepared and sterilized as described by Tolker-Nielsen and Sternberg
243 (Tolker-Nielsen and Sternberg, 2011). The substratum consisted of a microscope glass
244 coverslip (24 x 50 mm; KnittelGlasser, Braunschweig, Germany). Each channel was
245 inoculated with 250 µl of an overnight LB+Trim culture of *V. diazotrophicus* pFD086 diluted
246 (after 3 washing steps in MDV) to an OD_{600nm} of 0.1 in MDV. A 2h-attachment step was
247 performed without any flow of medium. Then a 5 $ml.h^{-1}$ flow of MDV was applied for 24 h
248 using a Watson Marlow 205U peristaltic pump (Watson Marlow, Falmouth, UK). Biofilms
249 were observed by monitoring the GFP fluorescence with a LSM 710 Confocal Laser Scanning
250 Microscope (Zeiss, Oberkochen, Germany) using a 40x oil immersion objective. GFP was
251 excited at 488 nm and fluorescence emission was detected between 500 and 550 nm.
252 Images were acquired at intervals of 1 µm throughout the whole depth of the biofilm. ZEN
253 2.1 software (Zeiss, Oberkochen, Germany) was used for visualization and image processing.
254 Quantitative analyses of image stacks were performed using COMSTAT software

255 (http://www.imageanalysis.dk/) (Heydorn et al., 2000). Analysis was performed from 3
256 biological replicates (independent experiments) and 8 technical replicates, every replicate
257 comprising 3 to 5 stacked images.
258
259 *Statistical analyses*
260 All statistical analyses were performed using GraphPad Prism; *p* values <0.05 were
261 considered statistically significant.
262
263 Phylogenomics, pangenomics and metagenomics detection of V. diazotrophicus NS1
264 We used anvi'o 7.1 (Eren et al., 2021) and the contigs snakemake (Koster and Rahmann,
265 2018) workflow with the heterotrophic bacterial diazotroph MAGs from Delmont et al.
266 (Delmont et al., 2022). Briefly, the workflow created a contigs database with "anvi-gen-
267 contigs-database," which used Prodigal version 2.6.3 (Hyatt et al., 2010) to identify open
268 reading frames. It used "anvi-run-hmm" to detect the single-copy core genes from bacteria
269 (n = 71, modified from (Lee, 2019)), ribosomal RNAs (rRNAs) (n = 12, modified from
270 https://github.com/tseemann/barrnap). For the phylogenomic tree of *V. diazotrophicus* NS1
271 and the MAGs from (Delmont et al., 2022), we selected 16 bacterial SCGs present in at least
272 40 out of the 41 genomes, which we concatenated and aligned using Muscle v3.8.1551
273 (Edgar, 2004) and used FastTree 2.1.11 (Price et al., 2010) to generate a tree. We used "anvi-
274 interactive" to visualize the phylogenomic tree.
275 To compare *V. diazotrophicus* NS1 with publicly available genomes of the same species, we
276 used "ncbi-genome-download" (https://github.com/kblin/ncbi-genome-download) to get all
277 *V. diazotrophicus* genomes from GenBank. We discarded two genomes for their very small
278 size. We used anvi'o Pangenomics snakemake workflow to compare the gene content
279 between the genomes. The workflow used Prodigal to identify open reading frames,
280 DIAMOND v2.0.14 (Buchfink et al., 2015) to quantify the similarity between each pair of
281 genes, the Markov Clustering Algorithm (MCL) to identify gene clusters, and Muscle
282 v3.8.1551 to align amino acid sequences. We used "anvi-compute-genome-similarity" to
283 compute the Average Nucleotide Identity (ANI) using pyANI v0.2.11 and visualized the
284 pangenome using "anvi-display-pan". We used the "functional homogeneity" index to filter
285 for more divergent gene clusters (max functional homogeneity of 0.95), which we used to

286 generate a *V. diazotrophicus* specific phylogenomic tree (n=99 genes) using the same
287 approach as described above (Muscle v3.8.1551 and FastTree 2.1.11).
288 We used COG20 (Galperin et al., 2021), KOfam (Aramaki et al., 2020) and the InterPro
289 website (Jones et al., 2014) to identify the nitrogen fixation associated genes. We extracted
290 three loci from each genome using "anvi-export-loci" and the anchor genes nifH (K02588),
291 nifU (K02594) and nifQ (K15790) and used the R package "gggenes"
292 (https://wilkox.org/gggenes/) to visualize the gene synteny.
293 We have also used metagenomes from the TARA ocean project to recruit reads on to *V.*
294 *diazotrophicus* NS1. Briefly, we use the "metagenomics" snakemake workflow in anvi'o and
295 mapped metagenomics short-reads using Bowtie2 (Langmead and Salzberg, 2012) and
296 summarized the results with `anvi-summarize`. We used the "detection" value to estimate
297 the presence/absence of V. diazotrophicus NS1 in both the prokaryotic and large size
298 fraction metagenomes.
299
300
301 **Results**
302
303 *Optimization of genetic tools for V. diazotrophicus NS1*
304
305 *V. diazotrophicus* NS1 is a marine strain, for which no genetic mutant has been described.
306 Because this strain might serve as an ideal model for genetic and ecophysiological
307 characterization of marine NCD, we sought to develop and optimize a genetic protocol for *V.*
308 *diazotrophicus* NS1. To achieve this aim, we first applied and modified an electroporation
309 protocol, originally developed for *Vibrio harveyi* and *Pseudoalteromonas* sp. (Delavat et al.,
310 2018). We tested different variants of the protocol, by using either 1- or 2 mm
311 electroporation cuvettes, modifying the voltage from 1500 to 2500 V in the presence or
312 absence of 15% glycerol in the sucrose buffer (Delavat et al., 2018), from stationary-phase
313 cultures grown in LB or LBS at 30°C. The best electroporation protocol yielded 81 CFU/µg
314 DNA, and was obtained when the following protocol was applied: glycerol-containing buffer
315 was used to wash LB-grown cultures, and the electroporation voltage was set at 2000 V in a
316 2 mm electroporation cuvette (data not shown). This demonstrates that, although being at
317 low efficiency, electroporation can be applied for this strain.

318 In order to improve the efficiency of exogenous DNA transfer to *V. diazotrophicus* NS1, we
319 also performed bi- and triparental mating as recently developed (Morot et al., 2021). Both
320 conjugations were successful for transferring the replicative plasmid pFD086 to *V.*
321 *diazotrophicus* NS1, giving rise to bright GFP-fluorescent cells (Figure 1). Finally, applying this
322 protocol, we successfully inserted a mini-Tn7 in *V. diazotrophicus* NS1 containing the
323 unstable pFD052 plasmid expressing the Tn7-transposase (Delavat et al., 2018), the latter
324 being subsequently cured (data not shown).
325
326 *Construction of a nifH deletion mutant and physiological characterization*
327
328 Unveiling the genetics and ecophysiology underlying diazotrophy in *V. diazotrophicus*
329 requires the deletion of genes and the subsequent physiological characterization of the
330 obtained mutants. In this study we focused on the deletion of the *nifH* gene
331 (BBJY01_570151), applying an adapted protocol successfully used for *V. harveyi* ORM4
332 (Morot et al., 2021). Using this protocol, a clean *nifH* deletion mutant was obtained (Figure
333 2A). This mutant does not show any growth phenotype when growing in LB-rich medium
334 (Figure 2B).
335 In order to characterize the diazotrophic activity of the *nifH* mutant, we developed a soft-
336 gellan assay, characterized by the use of a nitrogen-deprived medium containing 0.3% gellan
337 gum. Inoculating tubes sealed with a blue rubber stopper and an aluminum capsule (Figure
338 3) with *V. diazotrophicus* NS1 containing the empty plasmid pFD085 led to a growth of this
339 strain throughout the entire tube height (with a higher biomass closer to the surface) when
340 NH_4^+ is added. Importantly, in the absence of NH_4^+, a single ring is visible after 48h, located
341 around 15 mm below the surface of the medium. Applying this assay for the *nifH* mutant
342 containing pFD085 gave a similar pattern as the one of the wild type when grown with NH_4^+.
343 However, in the complete absence of nitrogen, no band nor growth was detectable in the
344 *nifH* mutant. Additionally, no band was visible when tubes were left for 2 more weeks,
345 indicating that the observed phenotype does not correspond to a longer lag phase in this
346 medium. *In trans* complementation of the *nifH* deletion mutant by the introduction by
347 conjugation of a replicative plasmid containing the entire *nifH* gene and its P_{nifH} promoter
348 restored the wild type phenotype, with the formation of a clear band located roughly 15 mm
349 below the surface of the medium (Figure 3). We subsequently repeated the experiment,

350 using NO_3^- as an alternative bioavailable nitrogen source, and the results were identical (see
351 Figure S1). Thus, we demonstrated that growth of *V. diazotrophicus* NS1 under nitrogen-
352 deprived medium is dependent on an intact nitrogenase.
353 The O_2 concentration in the soft-gellan tube was subsequently measured in the headspace
354 and at the location (or corresponding depth) of the growing ring. Uninoculated soft-gellan
355 tubes showed a high O_2 concentration at both locations, with values ranging from 173.6 µM
356 (sd 20.1) at a depth corresponding to the growing ring to 245.5 µM (sd 1.9) in the head
357 space. In contrast, after 72 hours growth of *V. diazotrophicus* in nitrogen-free MDV, the O_2
358 decreased to a concentration of 1.6 µM (sd 1.1) at the location of the ring, while this
359 concentration was 238.8 µM (sd 1.4) in the headspace. To better approximate the O_2
360 concentration at a depth where N_2 fixation can occur, we quantified this concentration in 12
361 hours-inoculated tubes, where the growing ring is not yet formed. Under this condition, a O_2
362 concentration of 14.8 µM (sd 7.7) is quantified at a similar depth as the one where the ring
363 will form 2 days later. Thus, we demonstrated here that diazotrophy occurs under
364 microaerobic conditions. Moreover, a subsequent soft-gellan experiment using *V.*
365 *diazotrophicus* NS1 constitutively expressing GFP (thanks to the pFD086 plasmid it contains)
366 showed that cells growing under microaerobic conditions within the ring are free-living and
367 isolated, and don't form aggregates (Figure S2).
368
369 *V. diazotrophicus* produces more biofilm in MDV
370
371 In order to determine the possible regulatory mechanism deployed by *V. diazotrophicus* NS1
372 to avoid the nitrogenase inhibition by O_2, we sought to quantify the ability of this strain to
373 produce biofilm. Microplates containing either LB, MDV or MDV supplemented with either
374 NO_3^- or NH_4^+, plus trimethoprim were inoculated with either *V. diazotrophicus* NS1 (pFD085),
375 *V. diazotrophicus* NS1 Δ*nifH* (pFD085) or *V. diazotrophicus* NS1 Δ*nifH* (pFD120), and left
376 without shaking at 30°C. Neither *V. diazotrophicus* NS1 nor their derivatives do produce any
377 biofilm when grown in LB. However, when grown in MDV, biofilm production significantly
378 increased in the three tested strains (Figure 4A), and this biofilm was located at the bottom
379 of the wells. Of note, the original MDV used for this experiment contains 100 $mg.l^{-1}$ yeast
380 extract, which provides low-but-necessary bioavailable nitrogen for the *nifH* mutant to grow,
381 allowing direct comparison of the 3 tested strains. Importantly, when MDV was

382 supplemented with NO_3^- or NH_4^+, the biofilm production significantly decreased as
383 compared to the one obtained in MDV medium. Additionally, we observed only subtle
384 differences between the different tested strains, all three of them producing more biofilm in
385 MDV as compared to LB and to MDV supplemented with either NO_3^- or NH_4^+. This increase in
386 biofilm formation in MDV suggests that in a nitrogen-limited medium, the production of
387 biofilm by *V. diazotrophicus* NS1 might protect its nitrogenase from an excess in O_2.
388 Furthermore, the thickness and biovolume of the biofilm produced in MDV by *V.*
389 *diazotrophicus* were quantified by confocal microscopy, using flow cells. Under this
390 condition, *V. diazotrophicus* produced an important biofilm (average biovolume of 11.70
391 $\mu m^3.\mu m^{-2}$, Standard Error of the Mean SEM 1.64 μm). The thickness of the biofilm was also
392 measured, reaching on average 26.65 μm (SEM 3.25 μm) and a maximal thickness of 46.35
393 μm (SEM 3.34 μm) after 24 hours (Figure 4BCD). After 48 hours, these values increased even
394 more, but the biofilm matrix was too dense and too heterogeneous, probably because of the
395 maturation of the biofilm, causing early dispersal (Supplementary Figure S3).
396
397 *V. diazotrophicus is different from recently discovered heterotrophic bacterial diazotrophs*
398
399 The genome of *V. diazotrophicus* NS1 was compared with the 40 Metagenome-Assembled
400 Genomes (MAGs) of HBDs recently retrieved from *Tara ocean* metagenomes (Delmont et al.,
401 2022). Expectedly, *V. diazotrophicus* NS1 falls in a group containing all MAGs affiliated to
402 *Gammaproteobacteria* (Figure 5A). However, the closest MAG (called HBD_Gamma_02 here
403 and in (Delmont et al., 2022)) seems to be affiliated to the order *Pseudomonales* and not to
404 *Vibrionales*, and ANI comparison (value of 0.68, see Table S4) confirmed their phylogenomic
405 distance. In addition, the genome of V. diazotrophicus NS1 was not detected in the Tara
406 ocean metagenomes (max detection was 8% of the genome, Table S5). We subsequently
407 compared the genomic relatedness of *V. diazotrophicus* NS1 to the genomes of 6 strains
408 isolated from deep subsurface sediments of the Baltic Sea (Castillo et al., 2018), to the one
409 isolated from phytoplankton exometabolite-enrichments (Fu et al., 2020) and to strain *V.*
410 *diazotrophicus* 99A isolated in Pennsylvania (unpublished data). Pangenomic and
411 phylogenomic analyses showed that *V. diazotrophicus* NS1 is closely related to 6 of these 8
412 strains (Figure 5B), with *V. diazotrophicus* 60.6B and HF9B standing a bit apart, possibly
413 belonging to a new species (ANIb comparison below 0.95, see Figure 5B and Table S4). Of

414 note, all of these nine *V. diazotrophicus* isolates carry a single copy of the *nifH* gene (Figure
415 5B and 5C) and a similar *nif* cluster (Figure 5C).
416
417 **Discussion**
418
419 Nitrogen fixation is a major metabolism in many ecosystems, supplying living micro- and
420 macro-organisms with otherwise scarce bioavailable nitrogen. In oceans, diazotrophy can
421 account for half of the annual new production in euphotic zones in oligotrophic oceans (Karl
422 et al., 1997). The diversity of marine diazotrophs has long been thought to be restricted to
423 members of the phylum *Cyanobacteria*. However, culture-independent approaches, like
424 those targeting the *nifH* gene or metagenomic and metatranscriptomic analyses from
425 various oceanic samples demonstrated the presence in abundance of non-cyanobacterial
426 diazotrophs (NCD, (Zehr et al., 1998; Delmont et al., 2018; Farnelid et al., 2019; Geisler et al.,
427 2019; Kapili et al., 2020; Delmont et al., 2022)). Despite these observations, few marine NCD
428 have been brought to culture (Farnelid et al., 2014; Martinez-Perez et al., 2018), hampering
429 in depth understanding of their ecophysiology and contribution to global N budget in
430 oceans. The goal of this study was to unveil the physiology of *V. diazotrophicus* NS1, a
431 marine NCD isolated already 40 years ago (Guerinot and Patriquin, 1981) but surprisingly
432 overlooked for in-depth analysis of its physiology.
433 The genome of *V. diazotrophicus* NS1 is available, and its analysis shows that it contains one
434 *nif* cluster, separated in 3 chromosomal locations and spanning some 110 Kbp (Figure 5C).
435 This cluster is found in all *V. diazotrophicus* strains whose genomes have been sequenced,
436 with only minor differences. The presence of only one *nif* cluster is unlike other soil NCD like
437 those belonging to the *Bradyrhizobium* genus, which can be endowed with 2 *nif* clusters (de
438 Matos et al., 2021). In line with this observation, we showed here that the *nifH* gene of all
439 sequenced *V. diazotrophicus* strains is part of the single-copy core gene fraction of the
440 genome (Figure 5C), unlike many other *Bradyrhizobium* strains (de Matos et al., 2021).
441 Because *V. diazotrophicus* NS1 belongs to one of the few marine NCD isolated, we sought to
442 develop and optimize genetic and molecular tools for this strain. Results show that *V.*
443 *diazotrophicus* is genetically tractable, both by electroporation and conjugation.
444 Electroporation efficiency was albeit low, as compared to the one reported for other *Vibrio*
445 or *Pseudoalteromonas* species (Delavat et al., 2018). Improving the electroporation

446 efficiency will require trials and errors, but having an already functional method reinforce its
447 high potential for rapid introduction of exogenous DNA, strengthened by its functionality in
448 other marine bacteria like *Algoriphagus machipongonensis* (Xu et al., 2022) or human
449 pathogens like *Vibrio parahaemolyticus* (Soree et al., 2022). Conjugation was more efficient,
450 both for the transfer of replicative plasmids and for the insertion of mini-transposons.
451 Mating is however more time-consuming and requires efficient counter-selection of the
452 donor. This counterselection is achieved here thanks to the use of strain β3914 (Le Roux et
453 al., 2007), a RP4+ and DAP-auxotroph strain, and thanks to a protocol recently optimized for
454 other *Vibrio* species (Morot et al., 2021).
455 In order to study the ecophysiology of marine NCD, we next focused on the targeted
456 deletion of genes. The *nifH* was the ideal candidate for gene deletion since it is found in only
457 one copy in *V. diazotrophicus* NS1, it is conserved in diazotrophs and considered as a
458 biomarker for diazotrophy and it codes the nitrogenase-reductase, and essential component
459 of the nitrogenase multiprotein complex. Adapting an already existing protocol (Morot et al.,
460 2021), we were able to perform a scarless deletion of the *nifH* gene in this strain. To our
461 knowledge, this mutant represents the first marine NCD mutant described in literature,
462 opening an avenue for a better characterization of their ecophysiology and role in the N and
463 C biogeochemical cycles. Its nitrogen-fixation capability was subsequently tested thanks to a
464 strain- and medium-adapted soft-gellan bioassay (Hashidoko et al., 2002; Hara et al., 2009).
465 This soft-gellan assay allows the inoculated bacteria to "find" their best appropriate O_2-
466 tension for optimized growth, characterized by a visible ring formed within the semi-solid
467 medium (Hashidoko et al., 2002). When nitrogen-free medium is used, the location of this
468 growing ring corresponds to the delicate balance between O_2 tension -necessary for aerobic
469 respiration- and diazotrophy inhibition by O_2. Additionally, gellan gum allows a complete
470 transparency of the medium and better visualization of bacterial growth (Hashidoko et al.,
471 2002), frequently allows faster growth and a higher bacterial diversity recovered (Tamaki et
472 al., 2009; Delavat et al., 2012; Delavat et al., 2013) and, importantly, bacteria grown in soft-
473 gellan show a much higher diazotrophic activity compared to the same bacteria grown in
474 soft-agar (Hara et al., 2009).
475 When grown in a nitrogen-free soft-gellan medium, we clearly showed that, unlike *V.*
476 *diazotrophicus* NS1 wild type, the Δ*nifH* mutant is unable to grow, while supplementing the
477 medium with NO_3^- or NH_4^+ as an organic nitrogen source allows its growth (Figure 3 and

478 Figure S1). Moreover, *in trans* complementation of the *nifH* mutant restores its capacity to
479 grow in a nitrogen-free medium, demonstrating that growth in this medium is dependent on
480 an intact nitrogenase. We also show here that the developed soft-gellan bioassay is powerful
481 to screen for diazotrophic activity and to phenotypically differentiate *V. diazotrophicus*
482 mutants, *e.g.* those related to N_2 fixation (catalytic or regulatory genes) or related to
483 protection from O_2. This experiment and the fact that no growth was obtained in the Δ*nifH*
484 mutant even after prolonged incubation in this soft-gellan tubes also confirm the presence
485 of only one copy of the *nifH* gene in the genome *V. diazotrophicus* NS1 and no paralog being
486 able to partially complement this mutation (Figure 5B).
487
488 Because of the inhibition of diazotrophy by O_2, nitrogen-fixation occurs at intermediate O_2
489 tension. We demonstrated here with a nitrogen-free soft-gellan medium that *V.*
490 *diazotrophicus* NS1 grows under microoxic conditions, ranging from 1 to 15 μM O_2 to
491 achieve a sufficient N_2 fixation activity to sustain its growth (Figure 3). Decreasing the local
492 O_2 tension is therefore important, and can be achieved by different means (for a review, see
493 (Gallon, 1992). As the ecophysiology of marine NCD is basically unknown, we tested whether
494 *V. diazotrophicus* NS1 is able to produce a biofilm, which would restrict the diffusion of O_2 in
495 the cells. Indeed, this strain produces more biofilm when grown in a nitrogen-limited
496 medium, compared with the biofilm formed in LB-rich medium (Figure 4A). This biofilm
497 formation decreases when NO_3^- or NH_4^+ is added as an alternative bioavailable nitrogen
498 source. These results were similar for the Δ*nifH* mutant and the Δ*nifH* complemented strain
499 (Figure 4A), demonstrating that biofilm production is not dependent on the presence of an
500 intact nitrogenase and that both processes are genetically decoupled, at least at this genetic
501 hierarchy. The thickness of the biofilm was quantified using flow cells, showing that *V.*
502 *diazotrophicus* NS1 produces a substantial biofilm after 24 hours of growth (Figure 4BCD).
503 The thickness of the biofilm measured in this experiment (on average of 26.65 μm) probably
504 serves as a barrier for O_2-diffusion. Indeed, this value is coherent with previous data,
505 showing the rapid decrease in O_2 in thick biofilms, which ultimately turn anoxic (Stewart et
506 al., 2016). Thus, *V. diazotrophicus* NS1 produces biofilm when grown under nitrogen-limited
507 condition, which might restrict O_2 diffusion, thus help solving the dilemma of nitrogenase
508 inhibition by O_2. This behaviour is analog to the one of the terrestrial strain *Pseudomonas*
509 *stutzeri* A1501, which produces biofilm under nitrogen-starved conditions (Wang et al.,

510 2017). Marine non cyanobacterial diazotrophs are in contrast less studied. Cell aggregates of
511 1-4 mm in diameter were observed for the marine diazotroph *P. stutzeri* BAL361 when
512 grown in nitrogen-free media under oxic condition, which was hypothesized to be an
513 adaptive mechanism for *P. stutzeri* BAL361 to fix N_2 despite high surrounding O_2-tension
514 (Bentzon-Tilia et al., 2015). Cell aggregation and exopolysaccharide production is also
515 suspected to play a role in the diazotrophic activity of the marine NCD *Sagittula castanea*,
516 even though cell aggregation was also observed under anoxic conditions in this strain
517 (Martinez-Perez et al., 2018). In this study, we showed that *V. diazotrophicus* cells grown
518 under microaerobic conditions in nitrogen-free media don't form aggregates (Figure S2), and
519 demonstrated an increase in biofilm density and biofilm thickness of a marine NCD when
520 grown under nitrogen-limited conditions as compared to LB-grown culture, constituting an
521 additional level of evidence that biofilm formation is important for these bacteria when
522 grown under oxic condition. This hypothesis is reinforced by the recent demonstration of the
523 high prevalence of marine NCD in high size fractions of marine metagenomic samples
524 (Delmont et al., 2022), suggesting NCD aggregation on particles and planktonic aggregates
525 (Farnelid et al., 2019; Geisler et al., 2019).
526 *V. diazotrophicus* is a bacterial species which has been isolated from different marine
527 environments, including sea water (Guerinot et al., 1982), gastrointestinal tractus of sea
528 urchin (Guerinot and Patriquin, 1981) or deep see sediments (Castillo et al., 2018), and from
529 enriched-phytoplankton exometabolites (Fu et al., 2020). However, this species is barely
530 detected from metagenomes coming from *Tara ocean* expeditions (Table S5), and is only
531 distantly related to newly discovered MAGs (Delmont et al., 2022). This almost absent
532 distribution from those metagenomic samples despite their effective presence in various
533 marine environments suggests that additional NCD live in alternative ecological niches that
534 have been overlooked by most metagenomic studies, like those from macroorganisms (*e.g.*
535 see urchins) or those from deep see sediment (Castillo et al., 2018).
536 In conclusion, this study allowed unveiling the ecophysiology of a marine NCD belonging to
537 the species *V. diazotrophicus*, which might serve as an ideal model to decipher their
538 ecological importance related to the N and C biogeochemical cycles and their genetic and
539 physiological adaptations to their environments, including the O_2-tension and the presence
540 of dissolved inorganic nitrogen.
541

Acknowledgments

The authors would like to thank Corentin Ramaugé-Parra for his help in the initial optimization of the genetic tools. The authors acknowledge the MicroScope plateform (https://mage.genoscope.cns.fr/microscope/home/index.php) for providing access to their plateform. This work was supported by the "Connect Talent" EpiAlg project awarded to Leila Tirichine, and by the "Rising Star" SMIDIDI project awarded to François Delavat, both from the French Pays de la Loire Region.

References

Aramaki, T., Blanc-Mathieu, R., Endo, H., Ohkubo, K., Kanehisa, M., Goto, S., and Ogata, H. (2020) KofamKOALA: KEGG Ortholog assignment based on profile HMM and adaptive score threshold. *Bioinformatics* **36**: 2251-2252.

Bentzon-Tilia, M., Severin, I., Hansen, L.H., and Riemann, L. (2015) Genomics and Ecophysiology of Heterotrophic Nitrogen-Fixing Bacteria Isolated from Estuarine Surface Water. *mBio* **6**: e00929.

Bombar, D., Paerl, R.W., and Riemann, L. (2016) Marine non-cyanobacterial diazotrophs: moving beyond molecular detection. *Trends Microbiol* **24**: 916-927.

Bonaldi, K., Gargani, D., Prin, Y., Fardoux, J., Gully, D., Nouwen, N. et al. (2011) Nodulation of *Aeschynomene afraspera* and *A. indica* by Photosynthetic *Bradyrhizobium* sp. Strain ORS285: The Nod-Dependent Versus the Nod-Independent Symbiotic Interaction. *Mol Plant-Microbe Interact* **24**: 1359-1371.

Buchfink, B., Xie, C., and Huson, D.H. (2015) Fast and sensitive protein alignment using DIAMOND. *Nat Methods* **12**: 59-60.

Capone, D.G., Burns, J.A., Montoya, J.P., Subramaniam, A., Mahaffey, C., Gunderson, T. et al. (2005) Nitrogen fixation by *Trichodesmium* spp.: An important source of new nitrogen to the tropical and subtropical North Atlantic Ocean. *Global Biogeochem Cycles* **19**: 1-17.

Carpenter, E.J., and Romans, K. (1991) Major role of the cyanobacterium *Trichodesmium* in nutrient cycling in the north atlantic ocean. *Science* **254**: 1356-1358.

Castillo, D., Vandieken, V., Engelen, B., Engelhardt, T., and Middelboe, M. (2018) Draft genome sequences of six *Vibrio diazotrophicus* strains isolated from deep subsurface Ssdiments of the Baltic Sea. *Genome Announc* **6**.

Cornejo-Castillo, F.M., and Zehr, J.P. (2019) Hopanoid lipids may facilitate aerobic nitrogen fixation in the ocean. *Proc Natl Acad Sci U S A* **116**: 18269-18271.

de Matos, G.F., Rouws, L.F.M., Simoes-Araujo, J.L., and Baldani, J.I. (2021) Evolution and function of nitrogen fixation gene clusters in sugarcane associated *Bradyrhizobium* strains. *Environ Microbiol.* **23**: 6148-6162.

Delavat, F., Lett, M.C., and Lièvremont, D. (2012) Novel and unexpected bacterial diversity in an arsenic-rich ecosystem revealed by culture-dependent approaches. *Biol Direct* **7**: art. 28.

Delavat, F., Lett, M.C., and Lievremont, D. (2013) Yeast and bacterial diversity along a transect in an acidic, As-Fe rich environment revealed by cultural approaches. *Sci Tot Environ* **463**: 823-828.

584 Delavat, F., Bidault, A., Pichereau, V., and Paillard, C. (2018) Rapid and efficient protocol to
585 introduce exogenous DNA in *Vibrio harveyi* and *Pseudoalteromonas* sp. *J Microbiol Methods*
586 **154**: 1-5.
587 Delmont, T.O., Quince, C., Shaiber, A., Esen, O.C., Lee, S.T., Rappe, M.S. et al. (2018)
588 Nitrogen-fixing populations of *Planctomycetes* and *Proteobacteria* are abundant in surface
589 ocean metagenomes. *Nat Microbiol* **3**: 804-813.
590 Delmont, T.O., Pierella Karlusich, J.J., Veseli, I., Fuessel, J., Eren, A.M., Foster, R.A. et al.
591 (2022) Heterotrophic bacterial diazotrophs are more abundant than their cyanobacterial
592 counterparts in metagenomes covering most of the sunlit ocean. *ISME J* **16**: 927-936.
593 Dixon, R., and Kahn, D. (2004) Genetic regulation of biological nitrogen fixation. *Nat Rev*
594 *Microbiol* **2**: 621-631.
595 Edgar, R.C. (2004) MUSCLE: multiple sequence alignment with high accuracy and high
596 throughput. *Nucleic Acids Res* **32**: 1792-1797.
597 Eren, A.M., Kiefl, E., Shaiber, A., Veseli, I., Miller, S.E., Schechter, M.S. et al. (2021)
598 Community-led, integrated, reproducible multi-omics with anvi'o. *Nat Microbiol* **6**: 3-6.
599 Farnelid, H., Harder, J., Bentzon-Tilia, M., and Riemann, L. (2014) Isolation of heterotrophic
600 diazotrophic bacteria from estuarine surface waters. *Environ Microbiol* **16**: 3072-3082.
601 Farnelid, H., Turk-Kubo, K., Ploug, H., Ossolinski, J.E., Collins, J.R., van Mooy, B.A.S., and Zehr,
602 J.P. (2019) Diverse diazotrophs are present on sinking particles in the North Pacific
603 Subtropical Gyre. *ISME J* **13**: 170-182.
604 Flores, E., Picossi, S., Valladares, A., and Herrero, A. (2019) Transcriptional regulation of
605 development in heterocyst-forming cyanobacteria. *Biochim Biophys Acta Gene Regul Mech*
606 **1862**: 673-684.
607 Foster, R.A., Kuypers, M.M., Vagner, T., Paerl, R.W., Musat, N., and Zehr, J.P. (2011) Nitrogen
608 fixation and transfer in open ocean diatom-cyanobacterial symbioses. *ISME J* **5**: 1484-1493.
609 Foster, R.A., Tienken, D., Littmann, S., Whitehouse, M.J., Kuypers, M.M.M., and White, A.E.
610 (2022) The rate and fate of N_2 and C fixation by marine diatom-diazotroph symbioses. *ISME J*
611 **16**: 477-487.
612 Fu, H., Smith, C.B., Sharma, S., and Moran, M.A. (2020) Genome Sequences and
613 Metagenome-Assembled Genome Sequences of Microbial Communities Enriched on
614 Phytoplankton Exometabolites. *Microbiol Resour Announc* **9**.
615 Gallon, J.R. (1992) Reconciling the Incompatible - N_2 Fixation and O_2. *New Phytol* **122**: 571-
616 609.
617 Galperin, M.Y., Wolf, Y.I., Makarova, K.S., Vera Alvarez, R., Landsman, D., and Koonin, E.V.
618 (2021) COG database update: focus on microbial diversity, model organisms, and
619 widespread pathogens. *Nucleic Acids Res* **49**: D274-D281.
620 Geisler, E., Bogler, A., Rahav, E., and Bar-Zeev, E. (2019) Direct detection of heterotrophic
621 diazotrophs associated with planktonic aggregates. *Sci Rep* **9**: 9288.
622 Goldberg, I., Nadler, V., and Hochman, A. (1987) Mechanism of nitrogenase switch-off by
623 oxygen. *J Bacteriol* **169**: 874-879.
624 Guerinot, M.L., and Patriquin, D.G. (1981) N_2-fixing vibrios isolated from the gastrointestinal
625 tract of sea urchins. *Can J Microbiol* **27**: 311-317.
626 Guerinot, M.L., West, P.A., Lee, J.V., and Colwell, R.R. (1982) *Vibrio diazotrophicus* sp. nov., a
627 marine nitrogen-fixing bacterium. *Int J Syst Bacteriol* **32**: 350-357.
628 Hara, S., Hashidoko, Y., Desyatkin, R.V., Hatano, R., and Tahara, S. (2009) High rate of N_2
629 fixation by east Siberian cryophilic soil bacteria as determined by measuring acetylene

630 reduction in nitrogen-poor medium solidified with gellan gum. *Appl Environ Microbiol* **75**:
631 2811-2819.
632 Hashidoko, Y., Tada, M., Osaki, M., and Tahara, S. (2002) Soft gel medium solidified with
633 gellan gum for preliminary screening for root-associating, free-living nitrogen-fixing bacteria
634 inhabiting the rhizoplane of plants. *Biosci Biotechnol Biochem* **66**: 2259-2263.
635 Heydorn, A., Nielsen, A.T., Hentzer, M., Sternberg, C., Givskov, M., Ersboll, B.K., and Molin, S.
636 (2000) Quantification of biofilm structures by the novel computer program COMSTAT.
637 *Microbiology-Sgm* **146**: 2395-2407.
638 Hubner, P., Willison, J.C., Vignais, P.M., and Bickle, T.A. (1991) Expression of regulatory *nif*
639 genes in *Rhodobacter capsulatus*. *J Bacteriol* **173**: 2993-2999.
640 Hyatt, D., Chen, G.L., Locascio, P.F., Land, M.L., Larimer, F.W., and Hauser, L.J. (2010)
641 Prodigal: prokaryotic gene recognition and translation initiation site identification. *BMC*
642 *Bioinform* **11**: 119.
643 Jones, P., Binns, D., Chang, H.Y., Fraser, M., Li, W., McAnulla, C. et al. (2014) InterProScan 5:
644 genome-scale protein function classification. *Bioinform* **30**: 1236-1240.
645 Kapili, B.J., Barnett, S.E., Buckley, D.H., and Dekas, A.E. (2020) Evidence for phylogenetically
646 and catabolically diverse active diazotrophs in deep-sea sediment. *ISME J* **14**: 971-983.
647 Karl, D., Letelier, R., Tupas, L., Dore, J., Christian, J., and Hebel, D. (1997) The role of nitrogen
648 fixation in biogeochemical cycling in the subtropical North Pacific Ocean. *Nature* **388**: 533-
649 538.
650 Karsenti, E., Acinas, S.G., Bork, P., Bowler, C., De Vargas, C., Raes, J. et al. (2011) A Holistic
651 Approach to Marine Eco-Systems Biology. *Plos Biol* **9**.
652 Kelly, M.J.S., Poole, R.K., Yates, M.G., and Kennedy, C. (1990) Cloning and mutagenesis of
653 genes encoding the cytochrome-bd terminal oxidase complex in *Azotobacter vinelandii* -
654 mutants deficient in the cytochrome-D complex are unable to fix Nitrogen in air. *J Bacteriol*
655 **172**: 6010-6019.
656 Koster, J., and Rahmann, S. (2018) Snakemake-a scalable bioinformatics workflow engine.
657 *Bioinform* **34**: 3600.
658 Landolfi, A., Kahler, P., Koeve, W., and Oschlies, A. (2018) Global Marine N_2 Fixation
659 Estimates: From Observations to Models. *Front Microbiol* **9**: 2112.
660 Langmead, B., and Salzberg, S.L. (2012) Fast gapped-read alignment with Bowtie 2. *Nat*
661 *Methods* **9**: 357-359.
662 Le Roux, F., Binesse, J., Saulnier, D., and Mazel, D. (2007) Construction of a *Vibrio splendidus*
663 mutant lacking the metalloprotease gene *vsm* by use of a novel counterselectable suicide
664 vector. *Appl Environ Microbiol* **73**: 777-784.
665 Lee, M.D. (2019) GToTree: a user-friendly workflow for phylogenomics. *Bioinform* **35**: 4162-
666 4164.
667 Martinez-Perez, C., Mohr, W., Schwedt, A., Durschlag, J., Callbeck, C.M., Schunck, H. et al.
668 (2018) Metabolic versatility of a novel N_2 -fixing Alphaproteobacterium isolated from a
669 marine oxygen minimum zone. *Environ Microbiol* **20**: 755-768.
670 Martinez-Perez, C., Mohr, W., Loscher, C.R., Dekaezemacker, J., Littmann, S., Yilmaz, P. et al.
671 (2016) The small unicellular diazotrophic symbiont, UCYN-A, is a key player in the marine
672 nitrogen cycle. *Nat Microbiol* **1**: 16163.
673 Mills, M.M., Turk-Kubo, K.A., van Dijken, G.L., Henke, B.A., Harding, K., Wilson, S.T. et al.
674 (2020) Unusual marine *cyanobacteria*/haptophyte symbiosis relies on N_2 fixation even in N-
675 rich environments. *ISME J* **14**: 2395-2406.

676 Morot, A., El Fekih, S., Bidault, A., Le Ferrand, A., Jouault, A., Kavousi, J. et al. (2021)
677 Virulence of *Vibrio harveyi* ORM4 towards the European abalone *Haliotis tuberculata*
678 involves both quorum sensing and a type III secretion system. *Environ Microbiol* **23**: 5273-
679 5288.
680 Mulholland, M.R., Bernhardt, P.W., Widner, B.N., Selden, C.R., Chappell, P.D., Clayton, S. et
681 al. (2019) High rates of N_2 fixation in temperate, Western North Atlantic coastal waters
682 expand the realm of marine diazotrophy. *Glob Biogeochem Cycles* **33**: 826-840.
683 Nieves-Morion, M., Flores, E., and Foster, R.A. (2020) Predicting substrate exchange in
684 marine diatom-heterocystous cyanobacteria symbioses. *Environ Microbiol* **22**: 2027-2052.
685 Nieves-Morion, M., Flores, E., Whitehouse, M.J., Thomen, A., and Foster, R.A. (2021) Single-
686 cell measurements of fixation and intercellular exchange of C and N in the filaments of the
687 heterocyst-forming Cyanobacterium *Anabaena* sp. strain PCC 7120. *mBio* **12**: e0131421.
688 Pamp, S.J., Sternberg, C., and Tolker-Nielsen, T. (2009) Insight into the microbial multicellular
689 lifestyle via flow-cell technology and confocal microscopy. *Cytometry A* **75**: 90-103.
690 Planes, S., Allemand, D., Agostini, S., Banaigs, B., Boissin, E., Boss, E. et al. (2019) The Tara
691 Pacific expedition-A pan-ecosystemic approach of the "-omics" complexity of coral reef
692 holobionts across the Pacific Ocean. *PLoS Biol* **17**: e3000483.
693 Poole, R.K., and Hill, S. (1997) Respiratory protection of nitrogenase activity in *Azotobacter*
694 *vinelandii* - Roles of the terminal oxidases. *Biosci Rep* **17**: 303-317.
695 Price, M.N., Dehal, P.S., and Arkin, A.P. (2010) FastTree 2--approximately maximum-
696 likelihood trees for large alignments. *PLoS One* **5**: e9490.
697 Sabra, W., Zeng, A.P., Lunsdorf, H., and Deckwer, W.D. (2000) Effect of oxygen on formation
698 and structure of *Azotobacter vinelandii* alginate and its role in protecting nitrogenase. *Appl*
699 *Environ Microbiol* **66**: 4037-4044.
700 Soree, M., Delavat, F., Lambert, C., Lozach, S., Papin, M., Petton, B. et al. (2022) Life-history
701 of oysters influence *Vibrio parahaemolyticus* accumulation in Pacific oysters (*Crassostrea*
702 *gigas*). *Environ Microbiol*.
703 Stewart, P.S., Zhang, T., Xu, R., Pitts, B., Walters, M.C., Roe, F. et al. (2016) Reaction-diffusion
704 theory explains hypoxia and heterogeneous growth within microbial biofilms associated with
705 chronic infections. *NPJ Biofilms Microbiomes* **2**: 16012.
706 Tamaki, H., Hanada, S., Sekiguchi, Y., Tanaka, Y., and Kamagata, Y. (2009) Effect of gelling
707 agent on colony formation in solid cultivation of microbial community in lake sediment.
708 *Environ Microbiol***11**: 1827-1834.
709 Tang, W., Wang, S., Fonseca-Batista, D., Dehairs, F., Gifford, S., Gonzalez, A.G. et al. (2019)
710 Revisiting the distribution of oceanic N_2 fixation and estimating diazotrophic contribution to
711 marine production. *Nat Commun* **10**: 831.
712 Tolker-Nielsen, T., and Sternberg, C. (2011) Growing and analyzing biofilms in flow
713 chambers. *Curr Protoc Microbiol* **Chapter 1**: Unit 1B 2.
714 Tuit, C., Waterbury, J., and Ravizza, G. (2004) Diel variation of molybdenum and iron in
715 marine diazotrophic cyanobacteria. *Limnol Oceanogr***49**: 978-990.
716 Wang, D., Xu, A., Elmerich, C., and Ma, L.Z. (2017) Biofilm formation enables free-living
717 nitrogen-fixing rhizobacteria to fix nitrogen under aerobic conditions. *ISME J* **11**: 1602-1613.
718 Xu, J., Ericson, C.F., Lien, Y.W., Rutaganira, F.U.N., Eisenstein, F., Feldmuller, M. et al. (2022)
719 Identification and structure of an extracellular contractile injection system from the marine
720 bacterium *Algoriphagus machipongonensis*. *Nat Microbiol* **7**: 397-410.

721 Zehr, J.P., Mellon, M.T., and Zani, S. (1998) New nitrogen-fixing microorganisms detected in
722 oligotrophic oceans by amplification of Nitrogenase (*nifH*) genes. *Appl Environ Microbiol* **64**:
723 3444-3450.
724 Zhang, C.C., Laurent, S., Sakr, S., Peng, L., and Bedu, S. (2006) Heterocyst differentiation and
725 pattern formation in *Cyanobacteria*: a chorus of signals. *Mol Microbiol* **59**: 367-375.
726

727

728 **Figure legend**

729

730 *Figure 1*

731 Microscopy picture showing the obtention of *V. diazotrophicus* carrying the GFP-expressing
732 plasmid pFD086. Images were acquired from LB-grown overnight cultures.

733

734 *Figure 2*

735 Genetic and physiological characterization of the *V. diazotrophicus* NS1 and the Δ*nifH*
736 mutant. (A) Gel electrophoresis showing the deletion of *nifH* in *V. diazotrophicus* NS1 (lanes
737 2 and 4). (B) Generation time of *V. diazotrophicus* NS1 and derivative mutants. *V.*
738 *diazotrophicus* NS1 and *V. diazotrophicus* NS1 Δ*nifH* contained the pFD085 plasmid and *V.*
739 *diazotrophicus* NS1 compl-*nifH* corresponds to *V. diazotrophicus* NS1 Δ*nifH* containing
740 pFD120. A one-way ANOVA with Tukey test was done to compare the different mutants.
741 Depicted here are the mean+SEM of 4 replicates.

742

743 *Figure 3*

744 Soft-gellan assay demonstrating bacterial growth under appropriate microoxic conditions.
745 The "+" and "-" indicate the presence or absence of NH_4^+, respectively. White arrows
746 indicate the location of the growing ring. Note the absence of ring in the Δ*nifH* mutant and
747 in the presence of NH_4^+. Similar results were obtained using NO_3^- as a bioavailable inorganic
748 nitrogen source (see Figure S1).

749

750 *Figure 4*

751 Biofilm formation characteristics of *V. diazotrophicus* NS1. (A) Corrected biofilm formation in
752 *V. diazotrophicus* NS1 and derivative mutants in different media. *V. diazotrophicus* NS1 and
753 *V. diazotrophicus* NS1 Δ*nifH* contained the pFD085 plasmid and *V. diazotrophicus* NS1

754 compl-*nifH* corresponds to *V. diazotrophicus* NS1 Δ*nifH* containing pFD120. Presented here
755 are the mean+SEM of at least three replicates. Significance was assessed by one-way ANOVA
756 with Tukey test for each mutant in the different media. (B) View of the top of the biofilm
757 produced by *V. diazotrophicus* NS1 pFD086 after 24 hours of incubation in a flow cell. (C)
758 Stacked microsopy image showing the thickness of the biofilm produced after 24 hours. (D)
759 Average and maximal thickness of the biofilm produced by *V. diazotrophicus* NS1 pFD086
760 after 24 hours. See Figure S3 for images corresponding to timepoint 48 hours.
761
762 **Figure 5. Comparative genomics of *V. diazotrophicus* NS1.** (A) Phylogenomics tree of *V.*
763 *diazotrophicus* NS1 and the 40 diazotroph MAGs from (Delmont et al., 2022) using 16 single
764 copy core genes occurring in at least 40 of the 41 genomes. We used FastTree to compute a
765 phylogenomic tree and anvi'o (Eren et al., 2021) for the visualization. (B) Pangenomics
766 analysis of publicly available *V. diazotrophicus*. A total of 6,928 gene clusters are represented
767 in the figure with each darker color in the genome's layer indicating the presence of gene
768 cluster in the corresponding genome. The red selection highlights the 2,884 single-copy core
769 genes. The heatmap corresponds to the ANI computed between all genomes and it is scaled
770 from below 0.95 ANI (white) to 1 ANI (dark red). We generated a phylogenomics tree (shown
771 above the ANI heatmap) using a subset of set of 99 single copy core gene with a maximum
772 functional homogeneity of 0.95 using anvi'o. (C) Conserved synteny of the *nif* gene locus
773 across multiple *V. diazotrophicus* genomes. The scale is based on the total size of the locus in
774 *V. diazotrophicus* NS1. The double bars indicates that the locus continues on a different
775 contig. Acc. Num: 65.7M (POSL00000000), 65.10M (POSM00000000), 60.27F
776 (POSK00000000), 60.18M (POSJ00000000), 60.6F (POSI00000000), 60.6B (POSH00000000),
777 HF9B (JAATOR000000000) and 99A (PRJNA456207).
778
779 *Supplementary Figure S1*
780 Soft-gellan assay demonstrating bacterial growth under appropriate microoxic conditions.
781 The "+" and "-" indicate the presence or absence of NO_3^-, respectively. White arrows
782 indicate the location of the growing ring. Note the absence of ring in the Δ*nifH* mutant and
783 in the presence of NH_4^+.
784
785 *Supplementary Figure S2*

786 Microscopy picture of *V. diazotrophicus* NS1 pFD086 cells grown under microoxic condition
787 in a nitrogen-free MDV soft-gellan medium. Cells from the growing ring were pipetted with a
788 syringe and a needle, and observed by epifluorescence microscopy. Please note that cells are
789 isolated and don't form aggregates.
790
791 *Supplementary Figure S3*
792 (A) View of the top of the biofilm produced by *V. diazotrophicus* NS1 pFD086 after 48 hours
793 of incubation in a flow cell. (B) three-dimensional representation showing the thickness of
794 the biofilm produced after 48 hours.
795

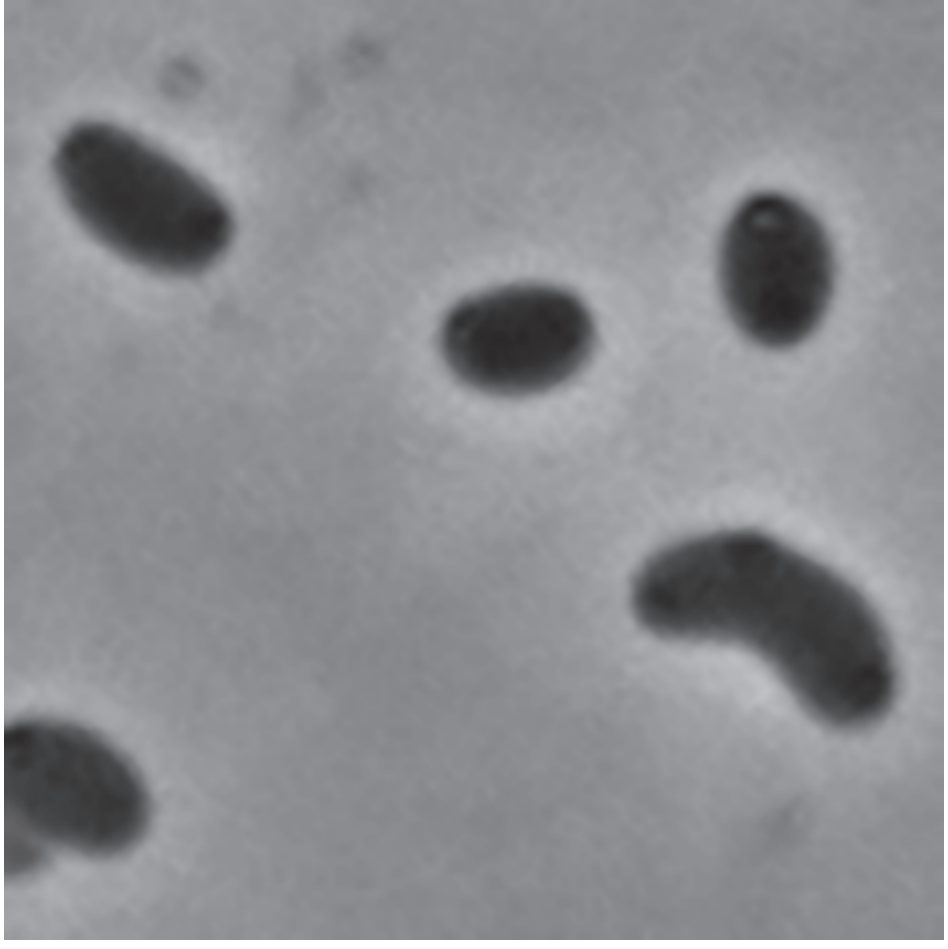

Phase Contrast

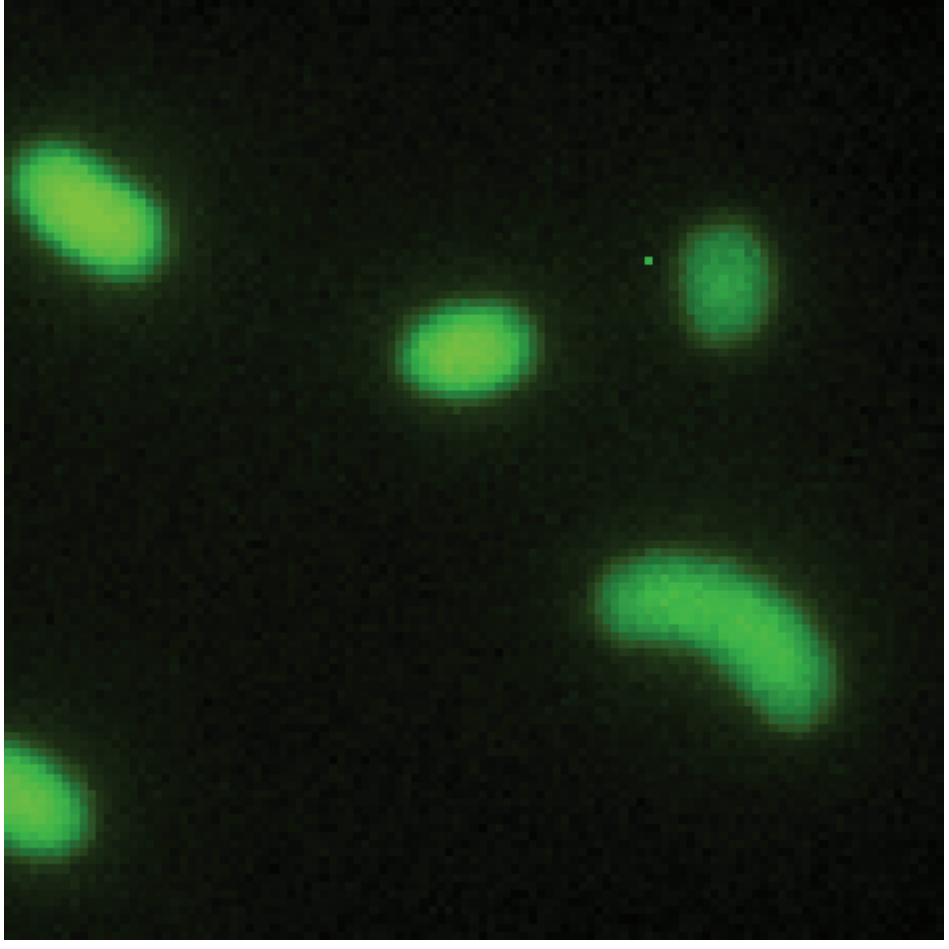

GFP

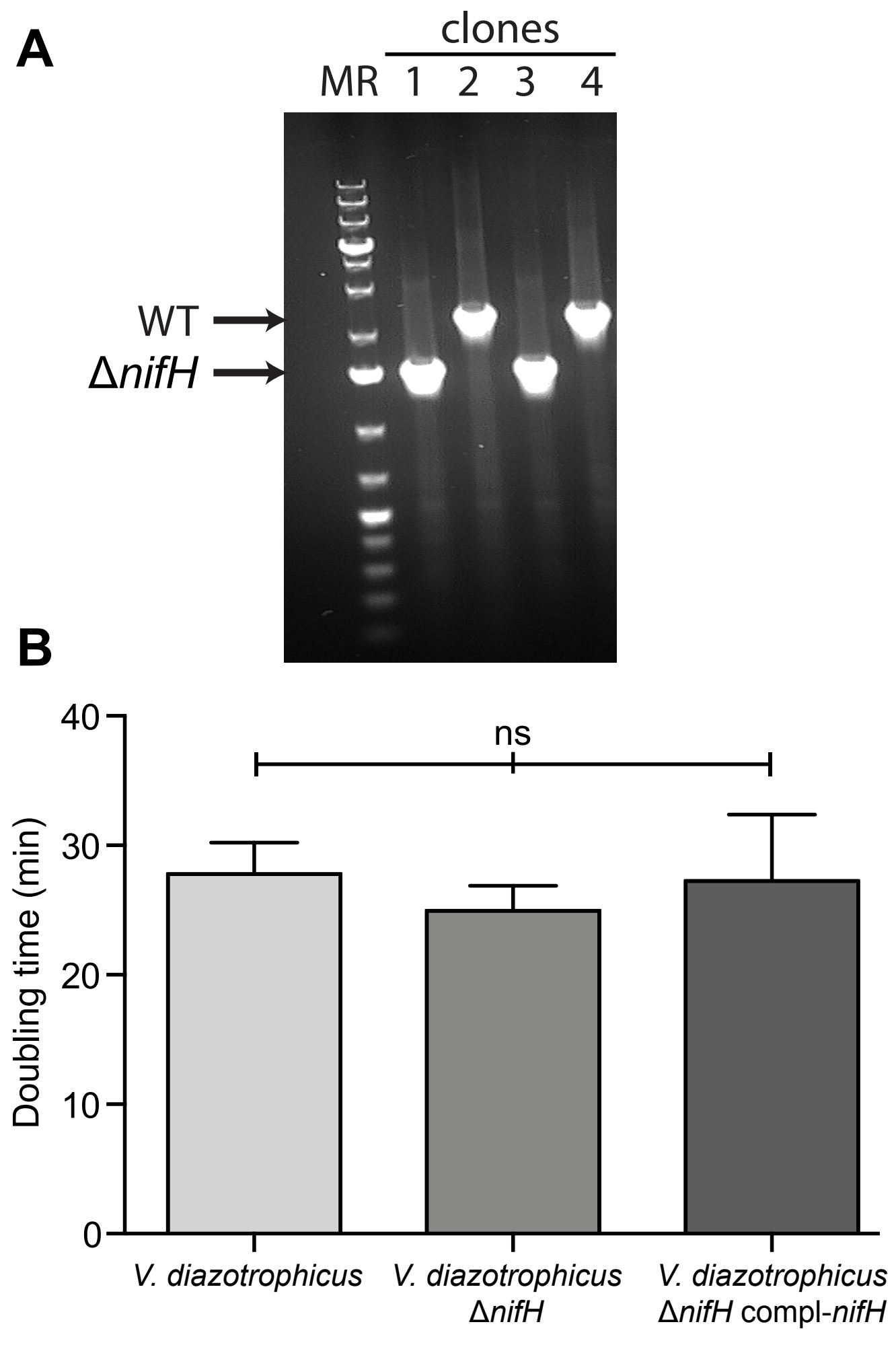
A
clones
MR
1
2
3
4
WT
ΔnifH
B
ns
Doubling time (min)
40
30
20
10
0
V. diazotrophicus
V. diazotrophicus ΔnifH
V. diazotrophicus ΔnifH compl-nifH

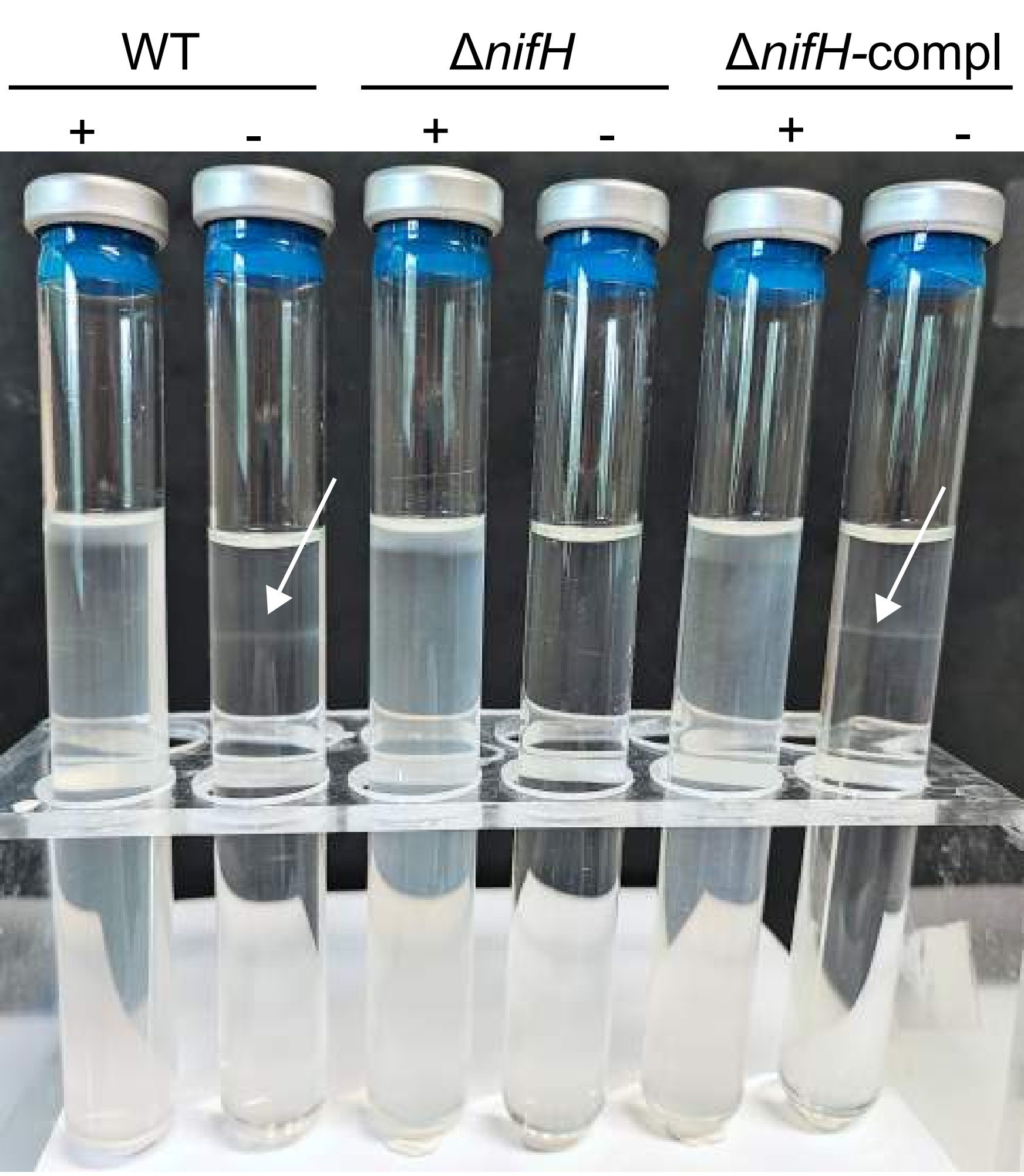
WT
Δ*nifH*
Δ*nifH*-compl
+
-
+
-
+
-

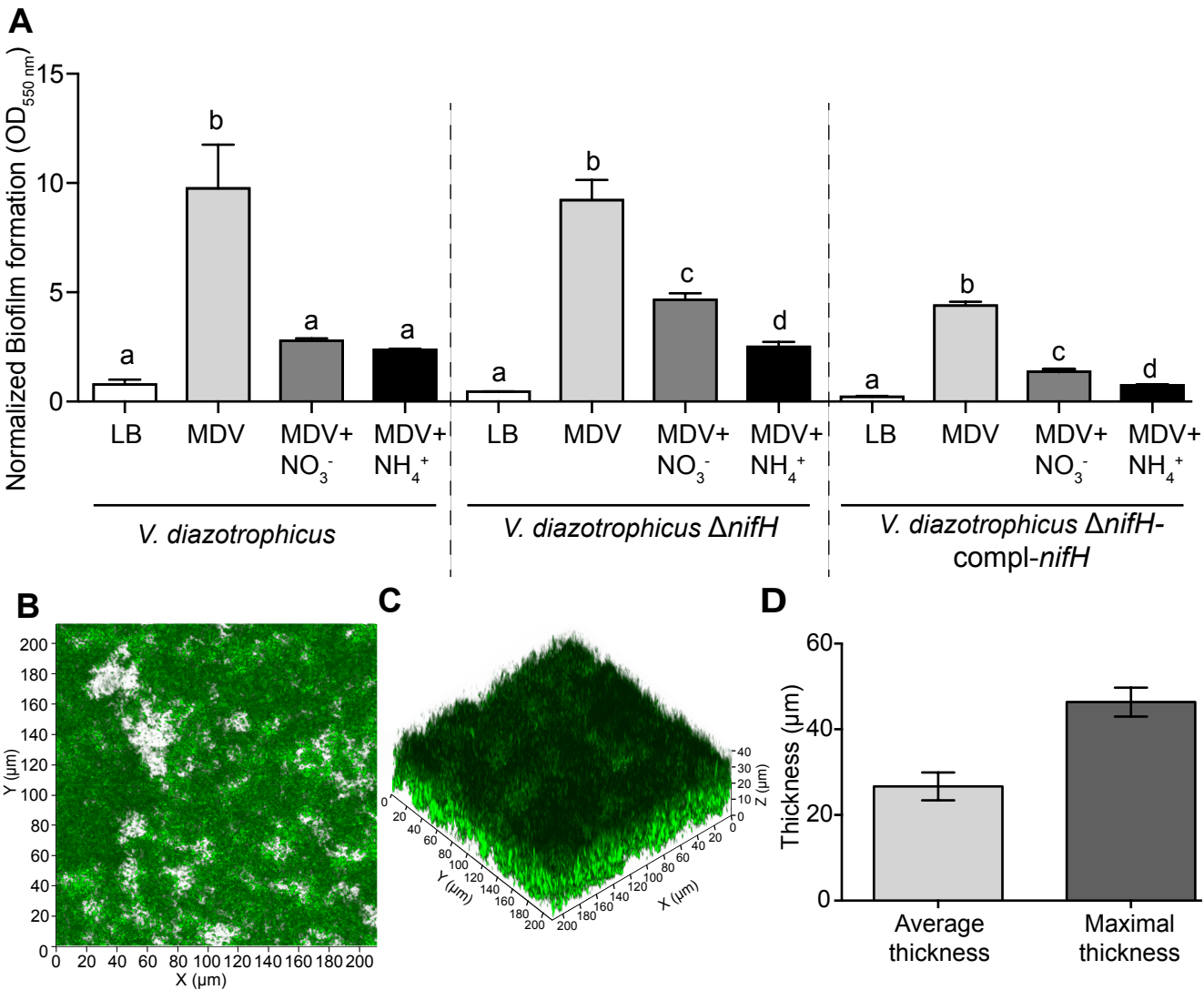
A
Normalized Biofilm formation ($OD_{550\ nm}$)
15
10
5
0
a
b
a
a
a
b
c
d
a
b
c
d
LB
MDV
MDV+ NO_3^-
MDV+ NH_4^+
LB
MDV
MDV+ NO_3^-
MDV+ NH_4^+
LB
MDV
MDV+ NO_3^-
MDV+ NH_4^+
V. diazotrophicus
V. diazotrophicus ΔnifH
V. diazotrophicus ΔnifH-compl-nifH
B
Y (µm)
X (µm)
C
Z (µm)
Y (µm)
X (µm)
D
Thickness (µm)
60
40
20
0
Average thickness
Maximal thickness

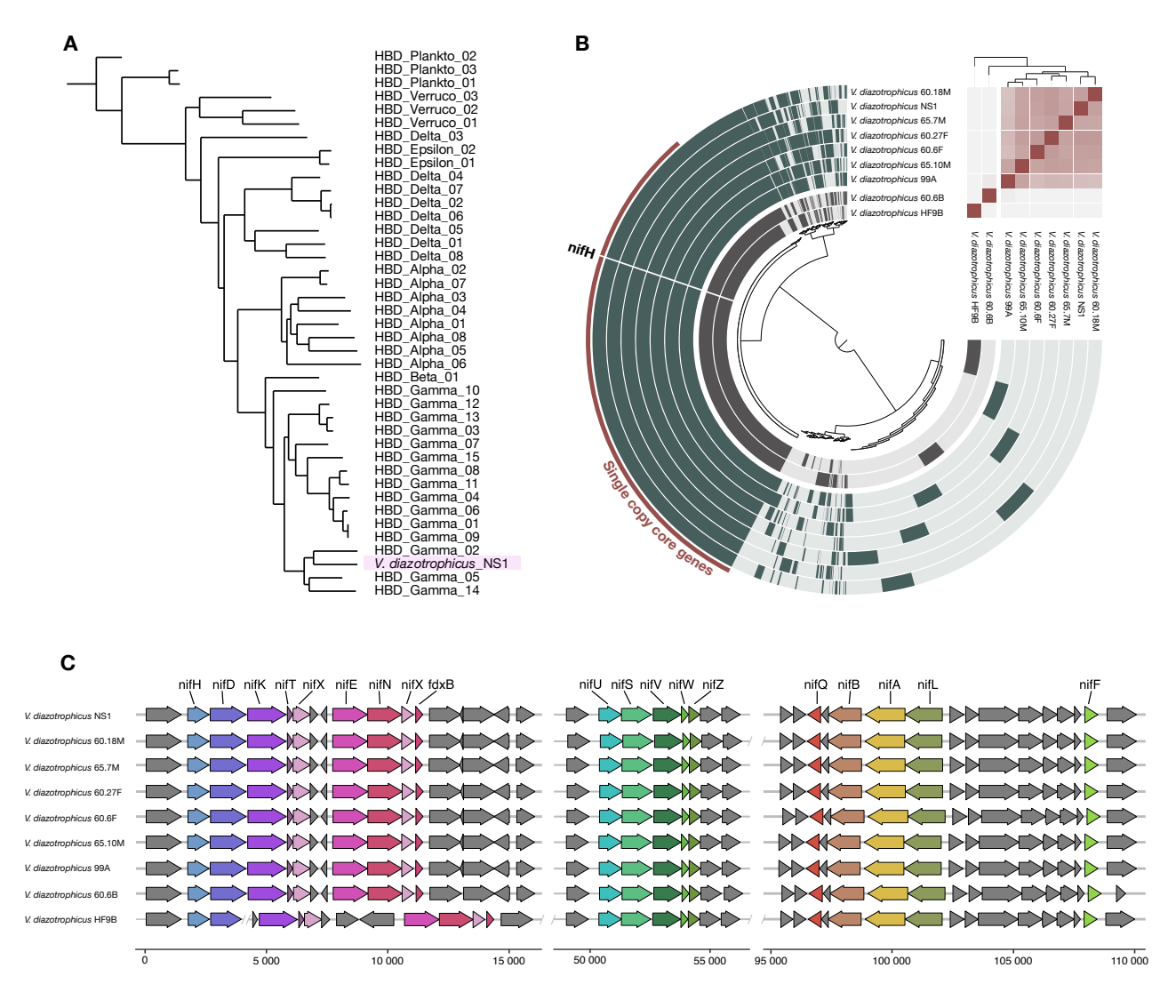
A
HBD_Plankto_02
HBD_Plankto_03
HBD_Plankto_01
HBD_Verruco_03
HBD_Verruco_02
HBD_Verruco_01
HBD_Delta_03
HBD_Epsilon_02
HBD_Epsilon_01
HBD_Delta_04
HBD_Delta_07
HBD_Delta_02
HBD_Delta_06
HBD_Delta_05
HBD_Delta_01
HBD_Delta_08
HBD_Alpha_02
HBD_Alpha_07
HBD_Alpha_03
HBD_Alpha_04
HBD_Alpha_01
HBD_Alpha_08
HBD_Alpha_05
HBD_Alpha_06
HBD_Beta_01
HBD_Gamma_10
HBD_Gamma_12
HBD_Gamma_13
HBD_Gamma_03
HBD_Gamma_07
HBD_Gamma_15
HBD_Gamma_08
HBD_Gamma_11
HBD_Gamma_04
HBD_Gamma_06
HBD_Gamma_01
HBD_Gamma_09
HBD_Gamma_02
V. diazotrophicus_NS1
HBD_Gamma_05
HBD_Gamma_14
B
V. diazotrophicus 60.18M
V. diazotrophicus NS1
V. diazotrophicus 65.7M
V. diazotrophicus 60.27F
V. diazotrophicus 60.6F
V. diazotrophicus 65.10M
V. diazotrophicus 99A
V. diazotrophicus 60.6B
V. diazotrophicus HF9B
nifH
Single copy core genes
C
nifH
nifD
nifK
nifT
nifX
nifE
nifN
nifX
fdxB
nifU
nifS
nifV
nifW
nifZ
nifQ
nifB
nifA
nifL
nifF
V. diazotrophicus NS1
V. diazotrophicus 60.18M
V. diazotrophicus 65.7M
V. diazotrophicus 60.27F
V. diazotrophicus 60.6F
V. diazotrophicus 65.10M
V. diazotrophicus 99A
V. diazotrophicus 60.6B
V. diazotrophicus HF9B
0
5 000
10 000
15 000
50 000
55 000
95 000
100 000
105 000
110 000